Macromolecules

Article

Cite This: *Macromolecules* 2018, 51, 7197−7208

pubs.acs.org/Macromolecules

Water Vapor Sorption, Diffusion, and Dilation in Polybenzimidazoles

Joshua D. Moon,[†,‡] Michele Galizia,[§] Hailun Borjigin,[∥] Ran Liu,[∥] Judy S. Riffle,[∥] Benny D. Freeman,*[,†,‡] and Donald R. Paul[†,‡]

[†]John J. McKetta Jr. Department of Chemical Engineering, The University of Texas at Austin, 200 E. Dean Keeton Street, Austin, Texas 78712, United States

[‡]Center for Energy and Environmental Resources, The University of Texas at Austin, 10100 Burnet Rd., Building 133 (CEER), Austin, Texas 78758, United States

[§]School of Chemical, Biological and Materials Engineering, The University of Oklahoma, 100 E. Boyd Street, Norman, Oklahoma 73019, United States

[∥]Department of Chemistry and Macromolecules Innovation Institute, Virginia Tech, Blacksburg, Virginia 24061, United States

S *Supporting Information*

ABSTRACT: Polybenzimidazoles (PBIs) have been investigated for use as gas separation membranes due to their thermal stability and good H_2/CO_2 separation performance at elevated temperatures. However, PBIs are hydrophilic, and effects of water vapor on PBI separation performance are essentially unexplored. This study investigates water sorption, diffusion, and dilation of a commercial PBI, Celazole, and a recently synthesized sulfonyl-containing PBI, TADPS-TPA. Water binds strongly to both polymers and requires elevated temperatures for removal. Water vapor sorption in Celazole follows dual-mode behavior up to unit activity, while upward concavity is observed at high activities in the TADPS-TPA sorption isotherm. Both PBIs swell significantly in water, and desorption hysteresis suggests water-induced conditioning of the PBI matrix. Model fits of dilation behavior enable estimation of partial molar volume and water-accessible fractional free volume (FFV) as a function of water activity. Water vapor diffusion coefficients increase with increasing vapor activity, which correlates with water-accessible FFV.

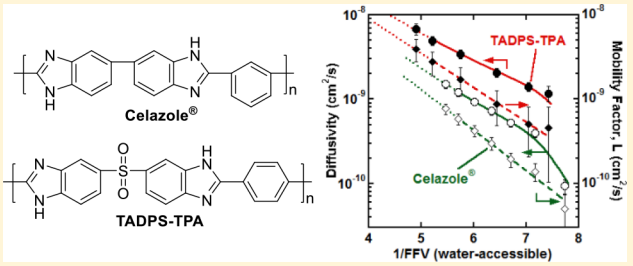

1. INTRODUCTION

Polybenzimidazoles (PBIs) are promising gas separation membranes. They have outstanding chemical, thermal, and mechanical stability, glass transition temperatures (T_g's) in excess of 400 °C, and decomposition temperatures approaching 600 °C.[1−8] Recent studies on PBIs have primarily targeted high-temperature H_2/CO_2 separations.[1,4,6,7] PBIs have permeabilities and selectivities near the 2008 Robeson upper bound at room temperature, and their separation performance at temperatures up to 250 °C can exceed the room temperature upper bound.[7,9,10] Many studies have focused on dense or asymmetric membranes formed from a commercial PBI, which is known as *m*-PBI or Celazole (cf. Figure 1).[1,4−6] A series of sulfonyl-containing PBIs based on a 3,3′,4,4′-tetraaminodiphenyl sulfone (TADPS) monomer were recently synthesized, and polymers from this series also exhibit outstanding thermal stability and mechanical properties.[8]

Unlike many polymers used for gas separation membranes, PBIs can sorb significant amounts of water (15−25 wt %).[8,11,12] Many industrial processes, such as syngas separation, operate with humidified gas streams, so it is important to understand the impact of sorbed water on membrane transport properties. Water may swell the polymer, disrupt hydrogen bonding between polymer chains, and fill free volume sites that would otherwise be available for gas sorption and transport.[13−15] Significant uptake of condensable vapors, such as water, could lead to swelling and plasticization, which can increase chain mobility and, in turn, increase penetrant diffusion coefficients, leading to increases in permeability and decreases in selectivity.[16−18] If the polymer segment relaxation rate is sufficiently low, as is often the case for glassy polymers,

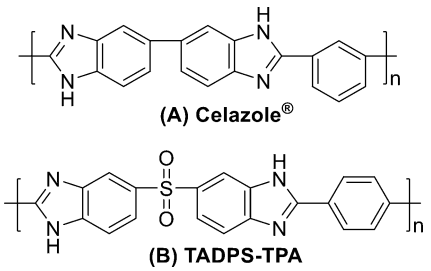

Figure 1. Molecular structures of (A) commercial PBI (Celazole) and (B) TADPS-TPA.[8]

Received: August 3, 2018
Revised: August 27, 2018
Published: September 10, 2018

DOI: 10.1021/acs.macromol.8b01659
Macromolecules 2018, 51, 7197−7208

the polymer may retain increased free volume after the swelling penetrant is removed, leading to conditioning.[16,19] Sorption of small amounts of bulky penetrants can cause antiplasticization, which reduces chain mobility and free volume, causing a decrease in penetrant diffusivities and an increase in polymer elastic modulus and strength.[16,20−22] The solubility of small molecules in polymers generally increases with increasing critical temperature, so highly condensable vapors can compete with less condensable gas molecules for sorption into Langmuir sites in glassy polymers, blocking sorption and transport of less condensable gases.[15,16,18,23−26]

In related studies, water vapor permeabilities in Matrimid 5218 and 6FDA-TMPDA polyimides increase with vapor activity at 35 °C.[27] CH_4 and CO_2 permeabilities in both polyimides decreased when water was present, with up to a 25−70% decrease at saturation, which was primarily attributed to competitive sorption.[27] Ansaloni et al. measured a similar decrease in permeabilities for CH_4, N_2, CO_2, and He in Matrimid. Specifically, at a water vapor activity of 0.75, gas permeabilities at 35 °C decreased by about 50% relative to pure gas permeabilities.[15] This effect correlated to a reduction in free volume caused by water occupying volume in the polymer matrix which would have otherwise been available for gas diffusion.[15] In contrast, Klaehn et al. reported that the presence of 2−4 vol % water increased permeabilities and activation energies of permeation of H_2, CH_4, and CO_2 in Matrimid at both 30 and 150 °C, with a corresponding decrease in gas selectivities.[28] While there are some discrepancies between these studies, they nonetheless illustrate the necessity of understanding the effects of contaminants, such as water, on gas separation performance of polymer membranes. Because PBIs exhibit 5−8 times the water uptake of Matrimid, it is important to understand the relative effects of water-induced plasticization, conditioning, antiplasticization, and competitive sorption on gas separation performance of PBI membranes.[8,11,12,29,30] However, to the best of the authors' knowledge, there are no studies in the literature describing these effects for PBIs.

This study reports water sorption, diffusion, and dilation in two representative polymers from the PBI family to explore the influence of water uptake on transport properties of PBIs. The first polymer considered is *m*-PBI, commercially available as Celazole. For comparison, a sulfonyl-containing PBI synthesized from 3,3′,4,4′-tetraaminodiphenyl sulfone and terephthalic acid, TADPS-TPA, is also considered. TADPS-TPA had the highest water uptake of three TADPS-based PBIs investigated in a prior study.[8] Thermal analysis of water populations in these PBIs was performed using thermogravimetric analysis (TGA) and differential scanning calorimetry (DSC). Water sorption and dilation isotherms were measured at 35 °C and are examined using the dual-mode sorption model. Differences in sorption behavior between Celazole and TADPS-TPA were correlated to polymer structure. The partial molar volumes of sorbed water and fractional free volumes of the water/polymer mixtures were estimated as a function of vapor activity. Finally, water vapor diffusion coefficients were determined.

2. EXPERIMENTAL METHODS

2.1. Materials. Celazole S26 dope solution was purchased from PBI Performance Products Inc. This solution contains 26% polymer solids dissolved in *N*,*N*-dimethylacetamide (DMAc) with 1.5 wt % LiCl added to enhance polymer solubility. TADPS-TPA was synthesized as described previously.[8] DMAc and *n*-heptane were purchased from Sigma-Aldrich and used without further purification. Deionized water was generated using a Millipore RiOS and A10 water purification system. Structures of Celazole and TADPS-TPA are shown in Figure 1.

2.2. Membrane Preparation. Dense TADPS-TPA films were formed via solution-casting as described previously.[8] Celazole films were cast using a similar technique after diluting the dope solution to 2 wt % polymer by adding DMAc and stirring overnight. The solution was filtered through a 0.45 μm PTFE filter and sonicated for 30 min to remove any bubbles. The solution was poured into a glass casting ring caulked to a glass plate and placed in a vacuum oven on a level surface. The solvent was removed by drying for at least 24 h under full vacuum at room temperature followed by 4 h at 80 °C and 1 h at 100 °C.[8] After the film was removed from the glass plate, it was boiled in deionized (DI) water for 4 h to remove residual DMAc. During the boiling step, the film was held between two pieces of metal mesh to prevent curling. The film was then soaked in DI water at room temperature for at least 24 h to remove LiCl. Removal of LiCl was verified by analyzing the desorption solution using ion chromatography. Finally, the film was dried under full vacuum at 140 °C for at least 24 h.[8] TGA was used to verify solvent removal.

2.3. Thermogravimetric Analysis. The temperature required to fully dry each PBI sample was analyzed via thermogravimetric analysis using a Q500 TGA instrument (TA Instruments) with a 60 mL/min dry N_2 purge (99.999% UHP grade from Airgas) and 10 °C/min ramp rate. The temperature was ramped to 35 °C and held for 48 h, then ramped to 100 °C and held for 12 h, and finally ramped to 150 °C and held for 12 h.

2.4. Differential Scanning Calorimetry (DSC). The states of sorbed water in Celazole and TADPS-TPA were analyzed via DSC using a Q100 DSC instrument (TA Instruments). Each PBI sample was soaked in DI water at 35 °C until equilibrated, then blotted, weighed, and transferred to an aluminum pan that was sealed and promptly loaded into the instrument. The DSC was purged during testing with a UHP N_2 blanket. The temperature was decreased to −80 °C at 10 °C/min, held for 5 min, and then increased to 150 °C at 10 °C/min. The temperature was held at 150 °C for 1 h to allow evaporation of most of the water from the sample, then cooled to −80 °C at 10 °C/min, and held for 5 min before another 10 °C/min ramp to 150 °C.

2.5. Water Vapor Gravimetric Sorption. Water vapor gravimetric sorption measurements were performed using a McBain quartz spring balance.[31,32] Small pieces of polymer, about 20−25 μm thick and a few square centimeters in area, were suspended from a sensitive quartz spring (Ruska Instrument Corporation) inside a water-jacketed glass chamber maintained at 35 °C. Thickness was measured using a digital micrometer (Mitutoyo, ±1 μm resolution). Prior to starting each test, the sample was degassed under full vacuum (<0.01 Torr) for a minimum of 3 days with a liquid nitrogen trap in the vacuum line. A glass reservoir containing DI water was used as a vapor generator. Prior to use, the water reservoir was degassed under vacuum to remove air and dissolved gases from the water. The vapor partial pressure was monitored using an MKS Baratron 626B transducer (full scale = 100 Torr, accuracy = 0.25% of full scale). The highest activity that could be reliably studied was around 0.65, since higher activities produced rapid condensation of water on any cold spots in the apparatus, leading to fluctuations in pressure readings and difficulty determining accurate vapor activities.

Interval sorption experiments were run by increasing the water vapor activity stepwise from 0 to 0.65 and then decreasing stepwise down to 0. Integral sorption measurements were also run to determine diffusion kinetics more accurately, where each sorption step was followed by a desorption step back down to 0 activity. The spring length was continuously monitored using a CCTV camera and IC Capture software (The Imaging Source), and the images were processed using ImageJ software.[33]

2.6. Water Vapor Dilatometry. Water vapor sorption-induced dilation was measured at 35 °C using an optical method. A long strip of polymer was suspended in the glass chamber used for sorption

DOI: 10.1021/acs.macromol.8b01659
Macromolecules 2018, 51, 7197−7208

measurements and gently held next to a guide rod using copper wire to prevent curling while permitting the sample to elongate freely. Sample dimensions were ~8 cm long × 0.3 cm wide with a thickness of ~20 μm. Samples were degassed at 35 °C under full vacuum for at least 24 h prior to starting each test. Interval dilation measurements were run by increasing water vapor activity stepwise from 0 to 0.65 and then decreasing stepwise down to 0. The length of the sample was continuously monitored using a CCTV camera and IC Capture software and analyzed using ImageJ. The change in sample length was converted into volumetric dilation as follows:[34−36]

$$\frac{\Delta V}{V_0} = \left(\frac{L}{L_{dry}}\right)^3 - 1 \quad (1)$$

where L is the dilated sample length, L_{dry} is the initial dry length, and $\Delta V/V_0$ is the fractional change in sample volume.

2.7. Liquid Water Uptake and Dilation. Liquid water uptake and polymer swelling upon exposure to liquid water (activity = 1) were measured. Three samples of each polymer with areas of a few square centimeters and thicknesses of ~20 μm were placed in glass scintillation vials and dried under vacuum for 4 days in a vacuum oven at 35 °C. The oven was then purged with air-dried via a column of Drierite, and the vials were immediately sealed upon opening the oven before transferring them to a balance to limit moisture uptake from the surrounding atmosphere. Because these vials sorbed some moisture after removal from the oven, the samples were quickly transferred to a new empty sealed vial that had been equilibrated at ambient humidity, the mass of which was subtracted from each measurement. The samples were returned to the vacuum oven in their original vials and dried for an additional day. They were then removed from the oven and transferred in sealed vials to a digital scanner. The surface areas of the films were determined using ImageJ after scanning the films.

The samples were then soaked in DI water for 5 days inside the oven maintained at 35 °C. Each sample was then removed, briefly blotted with paper tissue, and weighed immediately. The samples were soaked again in DI water at 35 °C overnight. Finally, they were removed, blotted, and measured again for their surface areas. The sample dilation in liquid water was estimated as follows:

$$\frac{\Delta V}{V_0} = \left(\frac{A}{A_{dry}}\right)^{3/2} - 1 \quad (2)$$

where A is the scanned area of the water-soaked sample and A_{dry} is the scanned area of the dry sample.

2.8. Density. Samples of Celazole and TADPS-TPA were dried in stainless steel Swagelok chambers equipped with isolation valves inside an oven under full vacuum at 35 °C for 6 days. The oven was purged with dry air via a Drierite column, and the isolation valves were immediately sealed upon opening the oven to prevent moisture from entering the chambers. The sealed chambers were transferred from the oven into a glovebox purged with dry nitrogen to maintain a humidity of <0.1% as measured by a digital hygrometer (Fisher Scientific, ±2% RH accuracy). The chambers were opened, and sample densities were determined using a balance equipped with a density kit (Mettler Toledo) inside the dry glovebox.[37] *n*-Heptane was used as the buoyant liquid due to its negligible sorption in PBIs over the time scale of the measurement, which was verified by soaking a sample in *n*-heptane for several days with no detectable mass change.

3. RESULTS AND DISCUSSION

3.1. Thermogravimetric Analysis. For both Celazole and TADPS-TPA, thermogravimetric analysis revealed that while most of the water sorbed from the atmosphere was removed at 35 °C, some water was tenaciously bound to the polymer backbone and could only be removed by heating the sample to higher temperatures. As shown in Figure 2 (top), there are two distinct mass losses when the temperature is ramped above 35 °C and held at 100 °C and then 150 °C. The amount of tenaciously bound water (i.e., water that cannot be removed under vacuum at 35 °C) in each PBI was calculated as the difference between the sample mass at the end of the 35 °C hold and the mass at the end of the 150 °C hold. The amounts of strongly bound water in Celazole and TADPS-TPA were 2.7 and 2.5 wt %, respectively. These water molecules likely interact with the PBI backbone via hydrogen bonds of sufficient strength that additional thermal energy is required to break them (cf. Figure 2 (bottom)). This result is consistent with other reports that PBIs retain some water at temperatures up to 150 °C even under full vacuum.[12,38] The same Celazole sample was tested twice, where the second scan was run several days after the sample had been re-exposed to ambient conditions. Because both curves are qualitatively similar, the mass loss is due to sorbed water from the atmosphere rather than chemical changes in the polymer or residual solvent from the casting procedure. This tenaciously bound water cannot be removed before the sorption and dilation experiments, since the equipment cannot operate at sufficiently high temperatures to completely dry the sample (i.e., 150 °C). The contribution of these water populations is not included in the water sorption values discussed below.

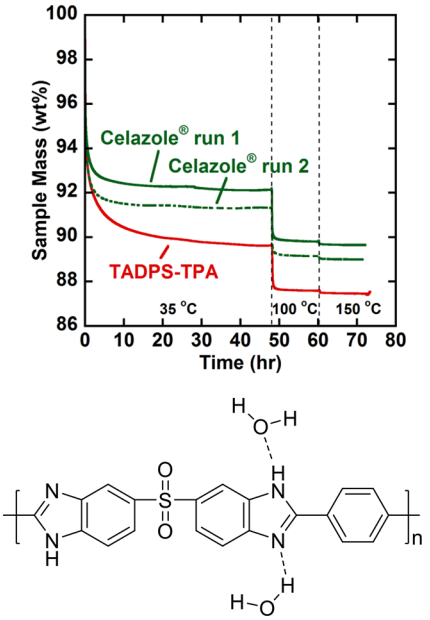

Figure 2. (top) TGA scans for Celazole (green curves) and TADPS-TPA (red curve). The first and second runs of Celazole are shown with solid and dashed lines, respectively. (bottom) Hypothesized water−PBI hydrogen-bonding interactions.[11,12,38−40]

3.2. Differential Scanning Calorimetry. Sorbed water in a hydrophilic polymer can exist in a distribution of states between free/mobile molecules and tightly bound molecules.[41−44] Free water has little interaction with the polymer chains and exhibits a melting point of 0 °C.[41−44] Loosely bound, freezable water interacts weakly with polymer chains or bound water molecules and exhibits a melting point below 0 °C.[41−44] Strongly bound water molecules will not exhibit any melting transition above −100 °C.[41−44] Previous studies have hypothesized that PBIs can undergo strong hydrogen-bonding interactions with water molecules due to the polar N and N−H groups on the polymer backbone (cf. Figure 2 (bottom)).[11,12,38−40] Tomlin et al. used X-ray crystallography on

DOI: 10.1021/acs.macromol.8b01659
Macromolecules 2018, 51, 7197−7208

a diimidazole model compound to conclude that water undergoes extensive hydrogen bonding with these functional groups and is even able to form bridges between benzimidazole groups.[38] Similar effects were observed during water vapor sorption in polyesters.[45] However, Brooks et al. used FTIR and broadline NMR to conclude that most of the sorbed water in PBI is not in fact bound to the polymer but is instead mobile inside the polymer matrix.[11]

First and second DSC heating scans of Celazole and TADPS-TPA saturated with DI water at 35 °C are shown in Figure 3 for the temperature range of −80 to 150 °C. For both

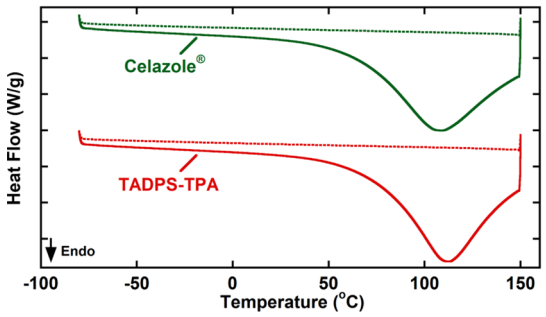

Figure 3. DSC scans of water-saturated Celazole (green curves) and TADPS-TPA (red curves). Solid curves represent the first heating scans, and dotted curves represent the second heating scans.

samples, there are no significant thermal transitions at or near 0 °C in the first heating ramps that would be indicative of melting mobile or freezable bound water molecules. Thus, essentially all of the sorbed water exists as strongly bound, nonfreezable molecules, which is consistent with the hypothesis that sorbed water interacts strongly with the PBI matrix via hydrogen bonding.[11,12,38−40] The broad endothermic peaks associated with water vaporization seen in the first heating scans are not present in the second ramps, indicating that most of the sorbed water was removed by holding at 150 °C for an hour after the first scan. A dedicated FTIR and DFT analysis is underway to identify the differences between tenaciously bound water (i.e., that not removed by drying at 35 °C) and other sorbed water populations as well as molecular level interactions of water with Celazole and sulfonyl-containing PBIs.

3.3. Water Vapor Sorption. Liquid water uptake at 35 °C in Celazole and TADPS-TPA are 19.8 ± 0.1 and 24.4 ± 0.1 wt %, respectively. These values are consistent with previous literature reports.[8,11,12] Water vapor sorption isotherms from interval measurements in Celazole and TADPS-TPA at 35 °C are shown in Figures 4A and 4B, where the mass uptake is given in grams of sorbed water per gram of dry polymer (i.e., dried at 35 °C). Sorption and desorption isotherms are shown for each material. Water vapor activities, or relative humidities, were evaluated as the ratio of water vapor partial pressure to its saturation pressure at 35 °C (i.e., $a = p/p^*$).[46] There was not a significant difference in water vapor uptake between Celazole and TADPS-TPA at lower activities, though TADPS-TPA showed higher vapor uptake than Celazole at high activities and 23% higher liquid water uptake. This result is possibly due to increased thermodynamic affinity between water and the sulfonyl groups or less steric hindrance from the *para*-linked

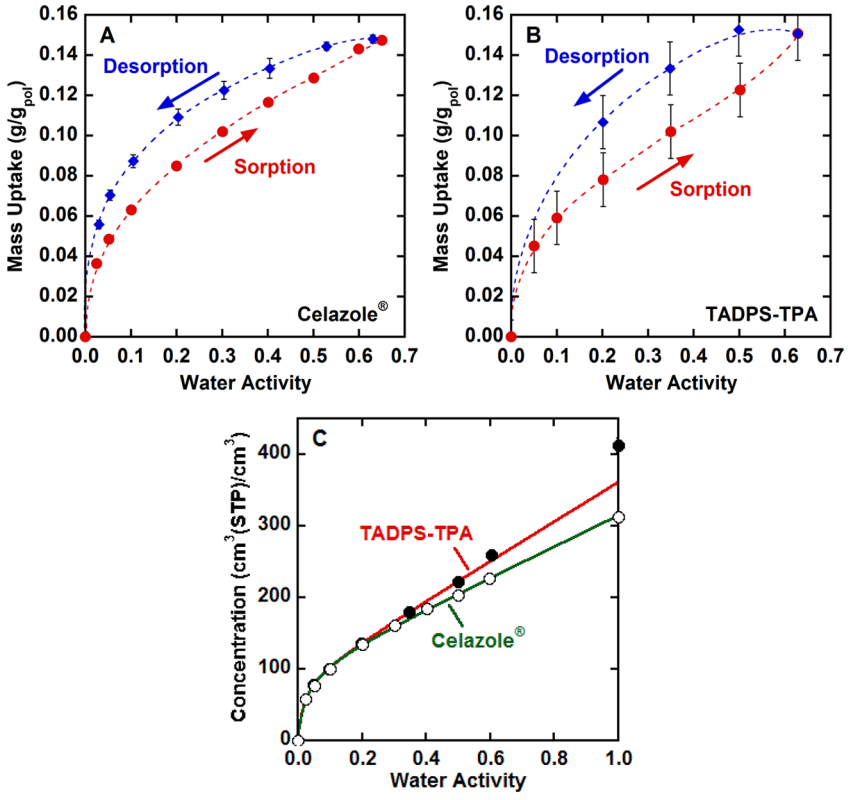

Figure 4. Water vapor sorption isotherms from interval measurements, expressed in g water per g dry polymer, in (A) Celazole and (B) TADPS-TPA at 35 °C. Dashed lines are guides for the eye. (C) Sorption isotherms for Celazole (open circles) from interval uptake steps and TADPS-TPA (solid circles) from integral uptake steps, expressed in cm^3 (STP) water per cm^3 dry polymer, with dual-mode model fits (red and green solid lines, respectively). The values at an activity of 1 were determined using liquid water uptake measurements. Error bars are too small to show.

DOI: 10.1021/acs.macromol.8b01659
Macromolecules 2018, 51, 7197−7208

Table 1. PBI Liquid Water Uptake and Dual-Mode Parameters for Water Vapor Sorption at 35 °C[a]

	k_D [cm^3 (STP)/cm^3·atm]	C'_H [cm^3 (STP)/cm^3]	b [atm^{-1}]	liquid uptake [wt %]	activity range
Celazole	3870 ± 140	102 ± 5	670 ± 90	19.8 ± 0.3	0−1.0
TADPS-TPA	4940 ± 380	88 ± 10	940 ± 470	24.4 ± 0.5	0−0.5
Celazole[51]	11780 ± 940	14 ± 28	240 ± 760	35	0−0.6
Kapton[50]	852	6.55	2011		N/A
Matrimid[29,30]	957			2.9−4.1	N/A
PEF[31]	354 ± 7	3.07 ± 0.4	141 ± 30		0−0.6
PET[31]	237 ± 16	0.599 ± 0.9	88.7 ± 180		0−0.6

[a]Sorption parameters reported for other polymers are at 35 °C with the exception of Kapton (30 °C) and Celazole (25 °C).[50,51]

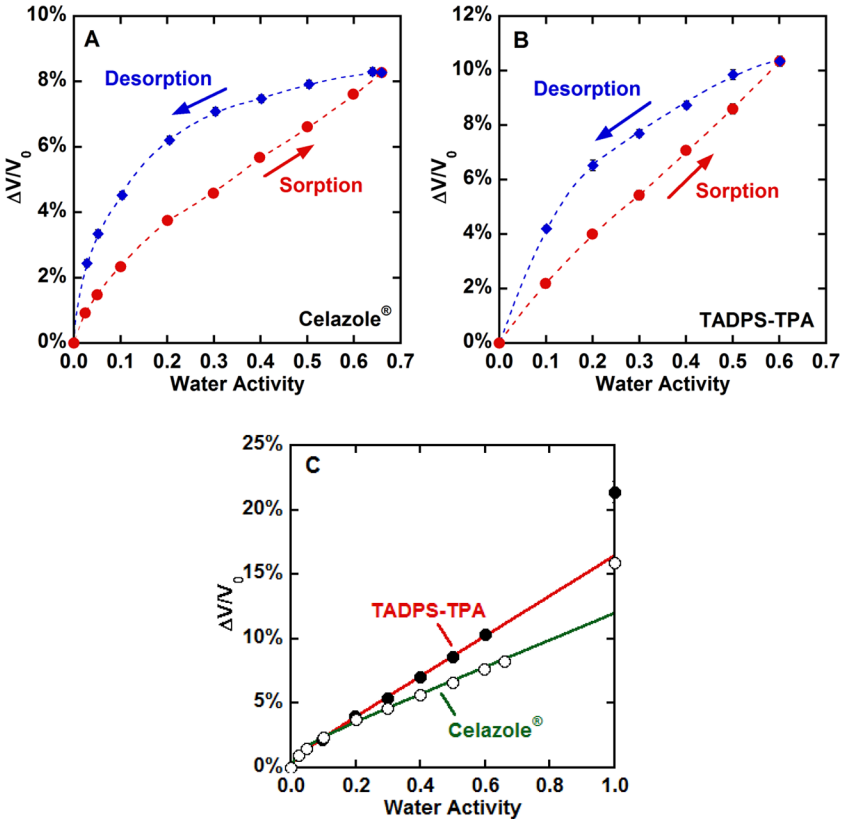

Figure 5. Water-induced dilation of (A) Celazole and (B) TADPS-TPA at 35 °C at activities up to about 0.6 from interval dilation measurements. Dashed lines are guides for the eye. Error bars are smaller than the symbols. (C) Water vapor dilation isotherms for Celazole (unfilled circles) and TADPS-TPA (filled circles) from uptake steps at 35 °C over the entire activity range. The values at unit activity were determined by immersion in liquid water. Solid lines are fits using eq 4 up to an activity of 0.5. Error bars are smaller than the symbols.

phenyl groups, allowing water to form hydrogen bonds more readily with the polar imidazole groups. A spectroscopic investigation is underway to elucidate the molecular origins of this behavior.

Significant hysteresis was observed during desorption experiments, suggesting that swelling may be occurring and that polymer chain relaxation is slow with respect to the desorption experiment time scale.[31] Similar behavior was observed by Burgess et al. for water vapor in poly(ethylene terephthalate) (PET) and poly(ethylene furanoate) (PEF) and by Schult and Paul for water vapor in poly(vinylpyrrolidone) (PVP), polysulfone (PSF), polyethyloxazoline (PEOX), and poly(ether sulfone) (PES).[31,47,48] The water uptake for both PBIs returns to zero after desorption, indicating that the sorption process is reversible.

Gas and vapor sorption isotherms in glassy polymers typically exhibit a concave-down behavior with pressure at low pressure or activity, which can be described using the dual-mode sorption model:[49]

$$C = k_D p + \frac{C'_H b p}{1 + b p} \quad (3)$$

where C is the sorbed gas or vapor concentration (cm^3 (STP)/cm^3), k_D is the Henry's law constant (cm^3 (STP)/cm^3·atm), C'_H is the Langmuir capacity (cm^3 (STP)/cm^3), and b is the Langmuir affinity (atm^{-1}). The equilibrium mass uptake of water at each sorption uptake step was converted to concentration (i.e., cm^3 (STP)/cm^3) using the polymer dry densities. Dry densities of 1.270 ± 0.014 g/cm^3 for Celazole and 1.362 ± 0.015 g/cm^3 for TADPS-TPA were determined as described earlier. The three dual-mode parameters (k_D, C'_H, and b) and their uncertainties were determined by a weighted least-squares regression of the sorption data via Mathematica and are summarized in Table 1. Values in the activity range of

DOI: 10.1021/acs.macromol.8b01659
Macromolecules 2018, 51, 7197−7208

0−1 were used for Celazole dual-mode fits, and values in the activity range of 0−0.5 were used for TADPS-TPA dual-mode fits. Numerical details of the fitting procedure are provided in the Supporting Information. Representative values for water vapor sorption in other glassy polymers are provided in Table 1 for comparison.[29−31,50,51] Fits of the water vapor sorption isotherms for Celazole and TADPS-TPA to the dual-mode model are shown in Figure 4C. The integral sorption values for TADPS-TPA and interval sorption values for Celazole were used for fitting as these experiments had the lowest experimental errors. Desorption behavior was not modeled due to additional complexities of hysteresis and conditioning, which are time-dependent phenomena.[52,53] Concentrations shown at unit activity are from liquid sorption measurements. Uncertainties were calculated using propagation of errors.[54]

The water vapor sorption isotherm for Celazole at 35 °C follows dual-mode behavior to unit activity, while the isotherm for TADPS-TPA follows dual-mode behavior approximately up to an activity of 0.5 (cf. Figures 4A and 4B). Both isotherms show similar behavior at low activities, while TADPS-TPA shows greater water uptake than Celazole at high activities. Celazole and TADPS-TPA have similar Langmuir capacities (C'_H) (cf. Table 1), which typically correlate with the amount of nonequilibrium excess free volume in the polymer.[55] This result is consistent with the similar fractional free volumes in both polymers, as discussed below. Both PBIs have higher Henry's law constants (k_D) than polyimides such as Kapton and Matrimid, possibly due to stronger water interactions with benzimidazole groups than imide groups, resulting in higher thermodynamic affinity. The lower Henry's law constants and liquid water uptake for Celazole than a previous reported measurement in the literature are likely due to differences in temperature and film casting procedure.[51] TADPS-TPA has both a higher Henry's law solubility (k_D) and Langmuir affinity (b) than those of Celazole, which may be due to the introduction of additional polar interactions with the sulfonyl group. An ongoing FTIR investigation may shed more fundamental light on these phenomena.

While the concave-down regions of the isotherms fit very well to the dual-mode model, a deviation from dual-mode behavior is observed at activities above 0.5 for TADPS-TPA, where an upturn occurs in the isotherm. This type II sorption isotherm behavior can be indicative of swelling of the polymer matrix or clustering of water molecules.[31,56] Similar behavior has been observed during water sorption in PET, PEF, Nafion, Kapton, polyacrylonitrile (PAN), *m*-HAB-6FDA, *m*-TR-450, and various polyarylates.[31,50,56−59] Previous studies have shown that PTMSP, PIM-1, 6FDA-TMPDA, *p*-HAB-6FDA, *p*-TR-450, and Matrimid exhibit linear to concave-up isotherms over the entire water vapor activity range.[26,27,30,59−61] The molecular origin of this behavior will be discussed below.

3.4. Water-Induced Swelling. Dilation experiments were performed to determine the swelling of the PBI matrices upon water vapor sorption. Swelling was isotropic, which was verified by measuring length and width changes of samples soaked in liquid water using a digital scanner. No anisotropy was observed for either PBI, which is consistent with both polymers being amorphous and unoriented.[8]

Celazole and TADPS-TPA swelled by 15.9 ± 0.1 and 21.4 ± 0.1 vol % in liquid water, respectively. The volumetric dilation of each PBI during water vapor sorption and desorption from interval measurements are presented in Figures 5A and 5B as a function of vapor activity. TADPS-TPA swells more than Celazole at higher vapor activities due to its higher water uptake. Similar to the sorption isotherms, significant hysteresis is observed for both PBIs, indicating that water is conditioning the polymers. This behavior is consistent with the very high glass transition temperatures of these PBIs (417 °C for Celazole and 480 °C for TADPS-TPA), which is indicative of low chain mobility.[8]

For CO_2 sorption in unconditioned polycarbonate, dilation was linear with pressure.[53] If sorption in Langmuir sites is treated as a purely hole-filling process, no additional chain separation would be required to accommodate penetrant sorption in the Langmuir mode.[53] In the ideal case, only penetrant molecules occupying Henry's law sites would contribute to swelling. However, Kamiya et al. reported that CO_2-induced dilation of polysulfone showed a concave-down behavior with pressure.[36] A similar concave-down behavior was observed by Fleming and Koros for CO_2 sorptive dilation in polycarbonate conditioned at high CO_2 pressure.[19] Kamiya et al. proposed an empirical model for dilation caused by gas sorption in glassy polymers that includes a contribution from swelling in both the Langmuir and Henry's law modes.[36] As shown by Punsalan and Koros, this model of dilation follows a similar functional form to the dual-mode sorption model:[36,62]

$$\frac{\Delta V}{V_0} = V_D\left(k_D p + \frac{fC'_H bp}{1 + bp}\right) \quad (4)$$

where $\frac{\Delta V}{V_0}$ is the fractional volume change from swelling, V_D is the effective condensed penetrant molar volume (cm^3/mol), and f is an empirical fitting parameter between 0 and 1 that describes the fraction of penetrant molecules sorbed in the Langmuir mode that contribute to polymer matrix dilation.

Interval dilation data from uptake steps in the activity range of 0−0.5 were fit to eq 4 using dual-mode parameters (k_D, C'_H, and b) from Table 1. Dilation data from desorption steps were not fit due to additional complexities of hysteresis and conditioning.[52,53] Dilation isotherms for TADPS-TPA and Celazole both deviate from linear behavior with activity and are well described by eq 4 up to an activity of 0.5 (cf. Figure 5C). The parameters V_D and f were determined by fitting dilation data to eq 4 using weighted least-squares regression of the dilation data from uptake steps via Mathematica and are recorded in Table 2. Dilation isotherms showed upward concavity at activities greater than ~0.6. More refined models than those in Figure 4 would be necessary to describe these effects.

Table 2. Parameters for Water-Induced Sorption Dilation of PBIs at 35 °C and Activities up to 0.5 Using Eq 4[a]

	V_D [cm^3/mol]	f
Celazole	10.8 ± 0.3	0.33 ± 0.03
TADPS-TPA	12.7 ± 0.5	0.17 ± 0.05

[a]Uncertainties were determined from Mathematica curve fitting.

3.5. Partial Molar Volume of Water. Sorption and dilation data were combined to estimate the partial molar volume of water in PBIs as a function of vapor activity or concentration. The partial molar volume ($\overline{V}_W$) of a sorbed penetrant in a polymer is defined as[35,63]

DOI: 10.1021/acs.macromol.8b01659
Macromolecules 2018, 51, 7197−7208

$$\bar{V}_W = \left(\frac{\partial V}{\partial n_W}\right)_{T,p,n_{j\neq i}} = \left[\frac{d}{dp}\left(\frac{\Delta V}{V_0}\right) + \beta\right]\frac{dp}{dC} \quad (5)$$

where $\Delta V/V_0$ is the polymer volumetric dilation and β is the polymer isothermal compressibility. Because penetrant-induced polymer swelling is much more significant than the isothermal compressibility, β can be neglected in eq 5.[35,64] The relationship between concentration and pressure is given by eq 3, and the relationship between dilation and pressure is given by eq 4.[36,49,62] The derivative of each with respect to pressure is given by

$$\frac{d}{dp}\left(\frac{\Delta V}{V_0}\right) = k_D V_D + \frac{fC'_H b V_D}{(1+bp)^2} \quad (6)$$

$$\frac{dC}{dp} = k_D + \frac{C'_H b}{(1+bp)^2} \quad (7)$$

Both derivatives can be substituted into eq 5 to yield the following expression for $\bar{V}_W$ as a function of pressure:

$$\bar{V}_W = V_D \frac{k_D + \frac{fC'_H b}{(1+bp)^2}}{k_D + \frac{C'_H b}{(1+bp)^2}} \quad (8)$$

Using the fitting parameters from Table 1, this equation can be used to calculate the partial molar volume of water as a function of its concentration in the polymer, which is shown in Figure 6. At low vapor activities, sorption occurs primarily in the Langmuir mode and results in little swelling and low partial molar volume values as the sorbed molecules are readily accommodated by existing excess free volume sites. The infinite dilution partial molar volumes of water in Celazole and TADPS-TPA are 4.0 and 2.8 cm^3/mol, respectively, far below the pure water molar volume (18 cm^3/mol). As concentration increases, these Langmuir sites become saturated, and sorption transitions from occurring primarily in Langmuir sites to occurring primarily in Henry's law sites, which results in more swelling and higher partial molar volumes. At high concentrations, the partial molar volume reaches a plateau when the excess free volume is saturated and no longer contributes to sorption. $\bar{V}_W$ approaches the effective molar volume of condensed penetrant at high activities (i.e., $\bar{V}_W \approx V_D$), which is 10.8 cm^3/mol for Celazole and 12.7 cm^3/mol for TADPS-TPA (cf. Table 2). These values are still substantially lower than the molar volume of 18 cm^3/mol for pure liquid water.[65] The partial molar volume of water in strong hydrogen-bonding solvents such as DMSO (15.6 cm^3/mol) and DMAc (14.2 cm^3/mol) is also lower than 18 cm^3/mol, which is thought to be due to the ability of water molecules to fit more readily into spaces between large solvent molecules than between other water molecules.[65] Similar behavior may be occurring at high water concentrations in PBIs.

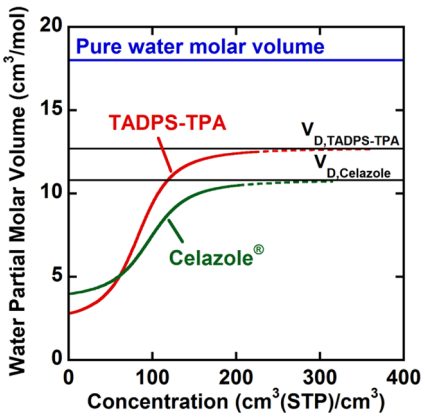

Figure 6. Partial molar volume of water vs water concentration in Celazole (green line) and TADPS-TPA (red line) calculated from dual-mode fitting parameters using eq 8. Dashed lines represent extrapolations beyond the data range used for fitting parameters (i.e., activities >0.5). Solid black lines represent effective molar volumes of condensed penetrant in each polymer (i.e., V_D).

For comparison, in 6FDA-ODA, $\bar{V}_W$ increased with concentration and reached a maximum of 0.011 nm^3/molecule (6.6 cm^3/mol) at saturation.[66] In UPJOHN 2080, a polyimide, $\bar{V}_W$ was 5.4 cm^3/mol at infinite dilution and increased to 13.8 cm^3/mol at high concentrations, which is qualitatively consistent with the observed values in Celazole and TADPS-TPA in Figure 6.[65] Similar behavior was also observed for water vapor in cellulose acetate.[65] Other literature studies report trends for the partial molar volume of small molecules in glassy polymers such as butane in PTMSP,[35] CO_2 in polycarbonate,[19,53,62] and methane and CO_2 in Matrimid,[62] consistent with the sigmoidal shape predicted by eq 8. This analytical approach to calculating partial molar volume could be generalized to other models of gas or vapor sorption and dilation in polymers, provided the models are differentiable.

3.6. Water Vapor Diffusion Kinetics. To determine whether the upward curvature in the TADPS-TPA sorption isotherm is due primarily to swelling or clustering, diffusion coefficients of water in the polymer were calculated as a function of vapor activity. Swelling would be expected to increase diffusion coefficients due to increased chain mobility, while clustering would decrease diffusion coefficients due to lower mobility of larger water aggregates.[31,56] A representative example of kinetic uptake data from a TAPDS-TPA integral sorption experiment is given in Figure 7A. Water vapor uptake kinetics can mostly be described using a Fickian diffusion model (cf. Figure 7A), but the data deviate from the model at short times, where there is a delay in uptake, and at long times, where an additional slow uptake mode is observed.[67] The curvature at short times is ascribed to a finite time required for water vapor to reach a constant concentration at the film surface after being introduced into the spring balance.[67−70] The analytical Fickian diffusion expression can be modified to account for varying surface concentration using an additional time constant, β.[67,68] The slower uptake behavior over long time intervals (i.e., a few hours to a couple of days) is ascribed to slow relaxation of the polymer. Following the method of Berens and Hopfenberg, this additional uptake can be accounted for by empirically adding an exponential relaxation term to the Fickian diffusion expression.[71] The resulting expression, including both the variable surface concentration and relaxation contributions, is provided in the Supporting Information. As shown in Figure 7A, this model agrees well with the experimental data. Diffusion coefficients were determined using weighted least-squares regression of the uptake data via Mathematica. Fitting parameters are provided in the Supporting Information.

As shown in Figure 7B, TADPS-TPA had higher water diffusion coefficients than Celazole over the entire activity range. Furthermore, water diffusion coefficients increased with

DOI: 10.1021/acs.macromol.8b01659
Macromolecules 2018, 51, 7197−7208

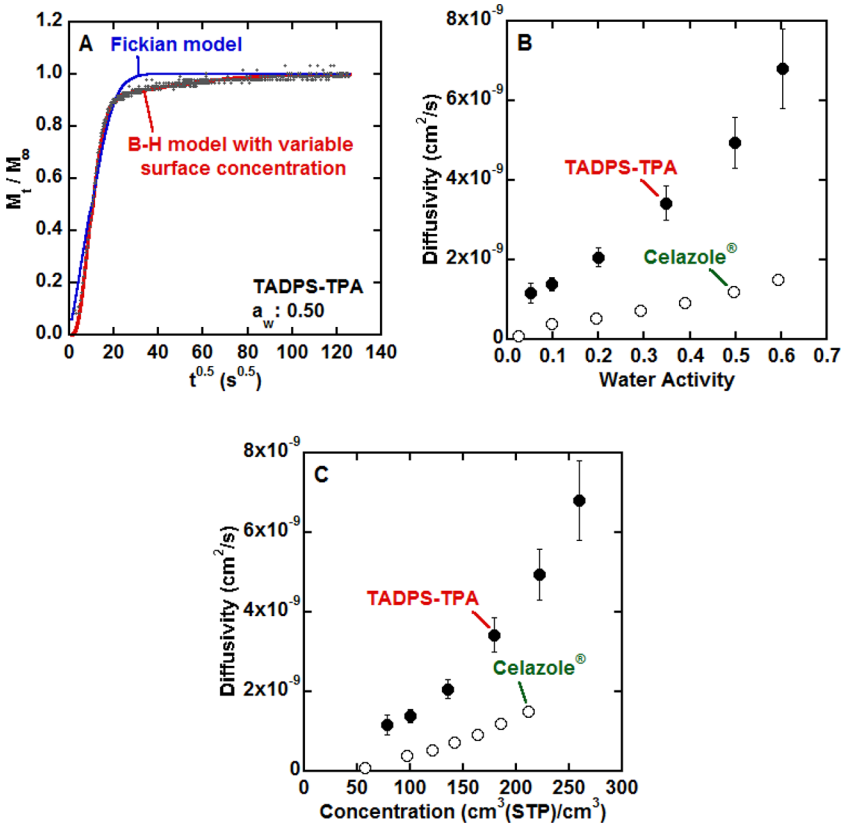

Figure 7. (A) Fractional mass uptake kinetics in TADPS-TPA at 35 °C during an integral water vapor sorption experiment at a final vapor activity of 0.5. Experimental values are shown as gray points, and Fickian and modified Berens–Hopfenberg (B–H) model fits are shown using blue and red solid lines, respectively. (B) Water vapor diffusion coefficients in Celazole (open circles) and TADPS-TPA (solid circles) at 35 °C as a function of vapor activity, calculated using the modified B–H model. (C) Water vapor diffusion coefficients in Celazole (open circles) and TADPS-TPA (solid circles) at 35 °C as a function of vapor concentration, calculated using the modified B–H model.[71]

water vapor activity (Figure 7B) and concentration (Figure 7C), so the upward concavity of the sorption isotherm is primarily due to swelling and plasticization of the polymer matrix rather than penetrant clustering. This result suggests that the water molecules are fairly uniformly dispersed throughout the polymer matrix, which is consistent with the lack of free water in the DSC scans. Similar increases in water vapor diffusivity at high concentrations due to plasticization have been observed for PET, PEF, and a series of polyarylates, while Kapton and PAN showed decreases in diffusivity that were attributed primarily to clustering.[31,50,56,58,72] The values of the relaxation rate constant, k_1, generally increased with increasing concentration for both polymers (cf. the Supporting Information).

Diffusion coefficients can be written as the product of a mobility coefficient (L), which is a purely kinetic factor accounting for the frictional resistance to penetrant transport, and a thermodynamic factor (α), which is related to polymer–penetrant interactions.[73−76] The thermodynamic factor for water in each PBI was calculated using dual-mode parameters and increased to a maximum of about 2.8 for both PBIs at a water weight fraction of ∼0.05 and then decreased at higher concentrations. The mobility factors correlated to the weight fraction of water in each PBI, indicating the increase in diffusivity for each PBI was mainly due to an increase in mobility rather than thermodynamic contributions. Higher mobility factors were observed for water vapor in TADPS-TPA than in Celazole, which suggests the higher diffusivities of TADPS-TPA are due to increased mobility in the polymer matrix rather than enhanced thermodynamic interactions with the polymer due to the introduction of the sulfonyl group.

While TADPS-TPA has a higher glass transition temperature than Celazole (480 °C vs 417 °C) that would typically indicate lower chain mobility at 35 °C, TADPS-TPA has a lower sub-T_g β transition than its sulfonyl-containing, *meta*-linked analogue, TADPS-IPA.[8] Increases in gas permeability for *para*-linked polyimides relative to their *meta*-linked counterparts have been hypothesized to result from enhanced rotational mobility of *para*-linked phenyl groups vs more restricted *meta*-groups.[77,78] Despite having a higher T_g, TADPS-TPA has higher gas permeabilities than *meta*-linked Celazole and TADPS-IPA, indicating sub-T_g motions may correlate more closely with penetrant mobilities than glass transition temperatures for these materials.[8] Further details of this analysis are provided in the Supporting Information.

3.7. Fractional Free Volume. Fractional free volume (FFV) is the fraction of volume inside a polymer that is not occupied by the polymer chains and is available to sorbed penetrants for diffusion. Gas permeability in glassy polymers depends exponentially on FFV, and a reduction in the number of available transient gaps between polymer segments leads to a drop in gas diffusivity (and vice versa).[79−81] A reduction in FFV can often lead to increased gas selectivities due to enhancement of the size-sieving ability of the polymer but at the cost of flux through the membrane. To determine how the FFV of PBIs may change in humid conditions, the expression

DOI: 10.1021/acs.macromol.8b01659
Macromolecules 2018, 51, 7197−7208

for FFV can be modified to account for changes in volume from water sorption and dilation. There are two approaches to calculating FFV as a function of humidity: either the volume occupied by water is excluded from the overall free volume or it is included. The first approach has been employed in correlating free volume changes with humidified gas permeabilities in Matrimid, where space occupied by water molecules is considered inaccessible for the diffusion of other molecules.[15] In that case, FFV is calculated as

$$\mathrm{FFV} = 1 - \frac{V_{0,\mathrm{poly}} - V_{0,\mathrm{w}}}{V} \tag{9}$$

The volume occupied by polymer chains ($V_{0,\mathrm{poly}}$) can be determined using group contribution methods, and the volume occupied by water ($V_{0,\mathrm{w}}$) can be estimated from water sorption data combined with either assumptions about the clustering of water in the polymer or direct measurements of water-induced dilation, if available.[15,82,83]

This first approach, however, provided unsatisfactory correlations between FFV and water vapor diffusion coefficients (see the Supporting Information). Diffusion coefficients often correlate with free volume according to eq 10:[79−81]

$$D = A \exp\left(-\frac{B}{\mathrm{FFV}}\right) \tag{10}$$

Equation 9 predicts a decrease in FFV at higher vapor concentrations (cf. Figure S2), which is inconsistent with the observed increase in diffusion coefficients.

An alternative approach to calculating FFV attempts to reconcile this discrepancy by considering the total volume accessible to water molecules for diffusion. Water molecules execute diffusion jumps between transient free volume elements as characterized by FFV. However, sorbed water molecules occupy some volume, the fraction of which increases with concentration. If both nonoccupied and water-occupied free volume elements are equally accessible for water diffusion, a "water-accessible" fractional free volume can be estimated as a function of concentration. In fractional form, this would be given by the following expression, which is similar to the FFV in eq 9 without the water-occupied volume term subtracted:

$$\mathrm{FFV}_{\text{water-accessible}} = 1 - \frac{V_{0,\mathrm{poly}}}{V} \tag{11}$$

Substitution of the appropriate expressions for $V_{0,\mathrm{poly}}$ and V into eq 11 yields the following expression:

$$\mathrm{FFV}_{\text{water-accessible}} = 1 - \frac{1.3\sum \hat{V}_{\mathrm{p}}^{\mathrm{vDw}}(1 - w_{\mathrm{w}})}{\hat{V}} \tag{12}$$

where $1.3\sum \hat{V}_{\mathrm{p}}^{\mathrm{vDw}}$ is the occupied volume of the polymer chains calculated using the van der Waals volumes of the polymer functional groups (cm^3/g), w_{w} is the weight fraction of water, and $\hat{V}$ is the specific volume of the water/polymer mixture (cm^3/g).[83] The values for $1.3\sum \hat{V}_{\mathrm{p}}^{\mathrm{vDw}}$ were determined to be 0.693 and 0.645 cm^3/g for Celazole and TADPS-TPA, respectively. The dry FFVs of Celazole and TADPS-TPA are 0.120 ± 0.010 and 0.122 ± 0.010, respectively, when w_{w} is equal to zero.

Two additional parameters needed to calculate water-accessible FFV are w_{w} and $\hat{V}$, both of which were determined from the sorption and dilation data. To evaluate water-accessible FFV using dual-mode parameters, the weight fraction of water can be calculated using eq S8. The specific volume of the water/polymer mixture is given by

$$\hat{V} = \frac{1 + \frac{\Delta V}{V_0}}{\rho_{\mathrm{dry}}\left(1 + \frac{18.02C}{22414\rho_{\mathrm{dry}}}\right)} \tag{13}$$

where ρ_{dry} is the dry density of the polymer (g/cm^3). By substituting eq 13 into eq 12 and using eqs 3 and 4 to describe the pressure dependence of concentration and dilation, respectively, we can evaluate water-accessible FFV as a function of activity or concentration using the five dual-mode sorption and dilation parameters, the dry density of the polymer, and the van der Waals volumes of the polymer segments from group contribution.

The resulting relationship between water-accessible FFV and concentration is given in Figure 8. The increase in water-accessible FFV is consistent with the increase in diffusion coefficient with concentration, as water-accessible FFV increases from 0.120 to 0.175 for Celazole and 0.122 to 0.192 for TADPS-TPA at 0.5 activity. Both Celazole and TADPS-TPA have similar water-accessible free volumes, which are dominated by nonoccupied volume at low concentrations and water-occupied volume at high concentrations. If the thermodynamic contribution to diffusion is removed, mobility factors for water transport in both polymers correlate linearly with inverse water-accessible FFV on a log scale, as shown in Figure 9. Based on these results, the increase in water mobility in PBIs is primarily due to an increase in accessible free volume from the significant amount of water sorption. Additional details on this analysis, including calculation of thermodynamic factors and mobility coefficients, are provided in the Supporting Information.

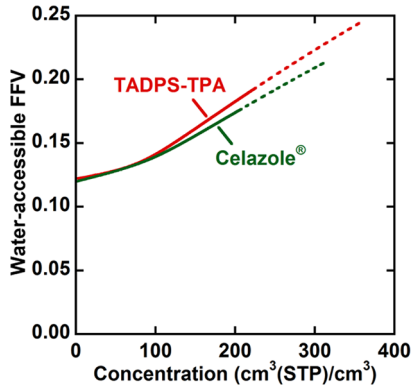

Figure 8. Water-accessible FFV vs water vapor concentration for Celazole (green line) and TADPS-TPA (red line) calculated from eq 12. Dashed lines represent extrapolations beyond the data range used for fitting parameters.

4. CONCLUSIONS

Water vapor sorption, diffusion, and dilation in two PBIs were investigated experimentally. Thermogravimetric analysis reveals that while most of the water sorbed by Celazole and sulfonyl-containing TADPS-TPA upon exposure to ambient conditions was removed by drying at 35 °C, an additional 2−3% of water tenaciously bound to the polymer backbone could only be removed at higher temperatures (i.e., 150 °C). Sorbed

DOI: 10.1021/acs.macromol.8b01659
Macromolecules 2018, 51, 7197−7208

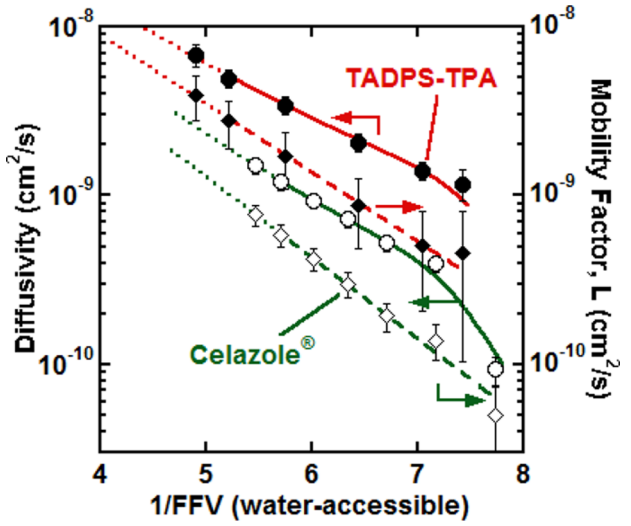

Figure 9. Water vapor diffusion coefficients and mobility factors, *L*, for water vapor in Celazole and TADPS-TPA. Open symbols and green curves are for Celazole, and solid symbols and red curves are for TADPS-TPA. Circles and diamonds are experimental diffusivities and mobility factors, respectively, and solid and dashed lines are corresponding model fits for *D* and *L*, respectively, based on eqs S7 and S12. Dotted lines represent extrapolations beyond the data range used for fitting parameters (i.e., activities >0.5).

water appears to be strongly bound to the PBI matrix, as evidenced by the lack of water melting transitions in DSC scans. Water vapor sorption isotherms for Celazole can be well-described by the dual-mode sorption model up to unit activity and for TADPS-TPA up to an activity of 0.5, with upward concavity occurring at higher activities. Both PBIs exhibit significant swelling upon exposure to water vapor, and TADPS-TPA exhibits both higher water solubility and more swelling than Celazole at higher activities. Water vapor diffusivities of both Celazole and TADPS-TPA increased with increasing vapor activity, which correlated to water-accessible fractional free volumes that include both non-occupied and water-occupied volume. The increase in diffusivities suggests that the effect of plasticization and swelling is more significant than penetrant clustering, which would tend to decrease diffusivities at high water vapor activity. TADPS-TPA has higher water vapor diffusivities than Celazole due to more swelling and greater chain mobility.

■ ASSOCIATED CONTENT

Supporting Information

The Supporting Information is available free of charge on the ACS Publications website at DOI: 10.1021/acs.macromol.8b01659.

Modified Berens−Hopfenberg diffusion equation and fitting parameters, weighted least-squares regression method, free volume models for water vapor diffusion, and calculation of mobility and thermodynamic factors for diffusion (PDF)

■ AUTHOR INFORMATION

Corresponding Author

*(B.D.F.) E-mail freeman@che.utexas.edu; Tel +1 (512) 232-2803.

ORCID

Joshua D. Moon: 0000-0002-4402-2362
Judy S. Riffle: 0000-0002-6291-6095
Benny D. Freeman: 0000-0003-2779-7788

Funding

This study was partially supported by the U.S. Department of Energy Office of Science, Office of Basic Energy Sciences under Award DE-FG02-02ER15362. We gratefully acknowledge partial support of this work by the Australian−American Fulbright Commission for the award to B.D.F. of the U.S. Fulbright Distinguished Chair in Science, Technology and Innovation sponsored by the Commonwealth Scientific and Industrial Research Organization (CSIRO). This material is based upon work supported in part by the National Science Foundation Graduate Research Fellowship Program under Grant DGE-1610403 and in part by the National Science Foundation under Cooperative Agreement EEC-1647722. Any opinions, findings, and conclusions or recommendations expressed in this material are those of the author(s) and do not necessarily reflect the views of the National Science Foundation.

Notes

The authors declare no competing financial interest.

■ REFERENCES

(1) Pesiri, D. R.; Jorgensen, B.; Dye, R. C. Thermal optimization of polybenzimidazole meniscus membranes for the separation of hydrogen, methane, and carbon dioxide. *J. Membr. Sci.* **2003**, *218*, 11−18.

(2) Kumbharkar, S. C.; Karadkar, P. B.; Kharul, U. K. Enhancement of gas permeation properties of polybenzimidazoles by systematic structure architecture. *J. Membr. Sci.* **2006**, *286*, 161−169.

(3) Kumbharkar, S. C.; Kharul, U. K. N-substitution of polybenzimidazoles: Synthesis and evaluation of physical properties. *Eur. Polym. J.* **2009**, *45*, 3363−3371.

(4) Kumbharkar, S. C.; Liu, Y.; Li, K. High performance polybenzimidazole based asymmetric hollow fibre membranes for H_2/CO_2 separation. *J. Membr. Sci.* **2011**, *375*, 231−240.

(5) Kumbharkar, S. C.; Li, K. Structurally modified polybenzimidazole hollow fibre membranes with enhanced gas permeation properties. *J. Membr. Sci.* **2012**, *415−416*, 793−800.

(6) Berchtold, K. A.; Singh, R. P.; Young, J. S.; Dudeck, K. W. Polybenzimidazole composite membranes for high temperature synthesis gas separations. *J. Membr. Sci.* **2012**, *415−416*, 265−270.

(7) Li, X.; Singh, R. P.; Dudeck, K. W.; Berchtold, K. A.; Benicewicz, B. C. Influence of polybenzimidazole main chain structure on H_2/CO_2 separation at elevated temperatures. *J. Membr. Sci.* **2014**, *461*, 59−68.

(8) Borjigin, H.; Stevens, K. A.; Liu, R.; Moon, J. D.; Shaver, A. T.; Swinnea, S.; Freeman, B. D.; Riffle, J. S.; McGrath, J. E. Synthesis and characterization of polybenzimidazoles derived from tetraaminodiphenylsulfone for high temperature gas separation membranes. *Polymer* **2015**, *71*, 135−142.

(9) Robeson, L. M. The upper bound revisited. *J. Membr. Sci.* **2008**, *320*, 390−400.

(10) Rowe, B. W.; Robeson, L. M.; Freeman, B. D.; Paul, D. R. Influence of temperature on the upper bound: Theoretical considerations and comparison with experimental results. *J. Membr. Sci.* **2010**, *360*, 58−69.

(11) Brooks, N. W.; Duckett, R. A.; Rose, J.; Ward, I. M.; Clements, J. An n.m.r. study of absorbed water in polybenzimidazole. *Polymer* **1993**, *34*, 4038−4042.

(12) Chung, T.-S. A Critical Review of Polybenzimidazoles. *Journal of Macromolecular Science, Part C* **1997**, *37*, 277−301.

(13) Catalano, J.; Myezwa, T.; De Angelis, M. G.; Baschetti, M. G.; Sarti, G. C. The effect of relative humidity on the gas permeability and

DOI: 10.1021/acs.macromol.8b01659
Macromolecules 2018, 51, 7197−7208

swelling in PFSI membranes. *Int. J. Hydrogen Energy* **2012**, *37*, 6308−6316.
(14) Giacinti Baschetti, M.; Minelli, M.; Catalano, J.; Sarti, G. C. Gas permeation in perflurosulfonated membranes: Influence of temperature and relative humidity. *Int. J. Hydrogen Energy* **2013**, *38*, 11973−11982.
(15) Ansaloni, L.; Minelli, M.; Giacinti Baschetti, M.; Sarti, G. C. Effect of relative humidity and temperature on gas transport in Matrimid®: Experimental study and modeling. *J. Membr. Sci.* **2014**, *471*, 392−401.
(16) Liu, Q.; Galizia, M.; Gleason, K. L.; Scholes, C. A.; Paul, D. R.; Freeman, B. D. Influence of toluene on CO_2 and CH_4 gas transport properties in thermally rearranged (TR) polymers based on 3,3′-dihydroxy-4,4′-diamino-biphenyl (HAB) and 2,2′-bis-(3,4-dicarboxyphenyl) hexafluoropropane dianhydride (6FDA). *J. Membr. Sci.* **2016**, *514*, 282−293.
(17) Chiou, J. S.; Barlow, J. W.; Paul, D. R. Plasticization of Glassy Polymers by CO_2. *J. Appl. Polym. Sci.* **1985**, *30*, 2633−2642.
(18) Yampolskii, Y.; Pinnau, I.; Freeman, B. D. *Material Science of Membranes for Gas and Vapor Separation*; John Wiley and Sons: New York, 2006.
(19) Fleming, G. K.; Koros, W. J. Carbon dioxide conditioning effects on sorption and volume dilation behavior for bisphenol A-polycarbonate. *Macromolecules* **1990**, *23*, 1353−1360.
(20) Maeda, Y.; Paul, D. R. Effect of antiplasticization on gas sorption and transport. I. Polysulfone. *J. Polym. Sci., Part B: Polym. Phys.* **1987**, *25*, 957−980.
(21) Maeda, Y.; Paul, D. R. Effect of antiplasticization on gas sorption and transport. III. Free volume interpretation. *J. Polym. Sci., Part B: Polym. Phys.* **1987**, *25*, 1005−1016.
(22) Omole, I. C.; Bhandari, D. A.; Miller, S. J.; Koros, W. J. Toluene impurity effects on CO_2 separation using a hollow fiber membrane for natural gas. *J. Membr. Sci.* **2011**, *369*, 490−498.
(23) Merkel, T. C.; Bondar, V.; Nagai, K.; Freeman, B. D. Sorption and transport of hydrocarbon and perfluorocarbon gases in poly(1-trimethylsilyl-1-propyne). *J. Polym. Sci., Part B: Polym. Phys.* **2000**, *38*, 273−296.
(24) Merkel, T. C.; Bondar, V.; Nagai, K.; Freeman, B. D.; Yampolskii, Y. P. Gas Sorption, Diffusion, and Permeation in Poly(2,2-bis(trifluoromethyl)-4,5-difluoro-1,3-dioxole-co-tetrafluoroethylene). *Macromolecules* **1999**, *32*, 8427−8440.
(25) Merkel, T. C.; Bondar, V. I.; Nagai, K.; Freeman, B. D.; Pinnau, I. Gas sorption, diffusion, and permeation in poly(dimethylsiloxane). *J. Polym. Sci., Part B: Polym. Phys.* **2000**, *38*, 415−434.
(26) Scholes, C. A.; Freeman, B. D.; Kentish, S. E. Water vapor permeability and competitive sorption in thermally rearranged (TR) membranes. *J. Membr. Sci.* **2014**, *470*, 132−137.
(27) Chen, G. Q.; Scholes, C. A.; Qiao, G. G.; Kentish, S. E. Water vapor permeation in polyimide membranes. *J. Membr. Sci.* **2011**, *379*, 479−487.
(28) Klaehn, J. R.; Orme, C. J.; Stewart, F. F.; Peterson, E. S. Humidified Gas Stream Separations at High Temperatures Using Matrimid 5218. *Sep. Sci. Technol.* **2012**, *47*, 2186−2191.
(29) Rowe, B. W.; Freeman, B. D.; Paul, D. R. Effect of Sorbed Water and Temperature on the Optical Properties and Density of Thin Glassy Polymer Films on a Silicon Substrate. *Macromolecules* **2007**, *40*, 2806−2813.
(30) Scholes, C. A.; Tao, W. X.; Stevens, G. W.; Kentish, S. E. Sorption of methane, nitrogen, carbon dioxide, and water in Matrimid 5218. *J. Appl. Polym. Sci.* **2010**, *117*, 2284−2289.
(31) Burgess, S. K.; Mikkilineni, D. S.; Yu, D. B.; Kim, D. J.; Mubarak, C. R.; Kriegel, R. M.; Koros, W. J. Water sorption in poly(ethylene furanoate) compared to poly(ethylene terephthalate). Part 1: Equilibrium sorption. *Polymer* **2014**, *55*, 6861−6869.
(32) Singh, A.; Freeman, B. D.; Pinnau, I. Pure and mixed gas acetone/nitrogen permeation properties of polydimethylsiloxane [PDMS]. *J. Polym. Sci., Part B: Polym. Phys.* **1998**, *36*, 289−301.
(33) Dhoot, S. N.; Freeman, B. D. Kinetic gravimetric sorption of low volatility gases and vapors in polymers. *Rev. Sci. Instrum.* **2003**, *74*, 5173−5178.
(34) Raharjo, R. D.; Freeman, B. D.; Sanders, E. S. Pure and mixed gas CH_4 and n-C_4H_{10} sorption and dilation in poly(dimethylsiloxane). *J. Membr. Sci.* **2007**, *292*, 45−61.
(35) Raharjo, R. D.; Freeman, B. D.; Sanders, E. S. Pure and mixed gas CH_4 and n-C_4H_{10} sorption and dilation in poly(1-trimethylsilyl-1-propyne). *Polymer* **2007**, *48*, 6097−6114.
(36) Kamiya, Y.; Hirose, T.; Naito, Y.; Mizoguchi, K. Sorptive dilation of polysulfone and poly(ethylene terephthalate) films by high-pressure carbon dioxide. *J. Polym. Sci., Part B: Polym. Phys.* **1988**, *26*, 159−177.
(37) Halliday, D.; Resnick, R.; Walker, J. *Fundamentals of Physics*; John Wiley & Sons: 2010.
(38) Tomlin, D. W.; Fratini, A. V.; Hunsaker, M.; Wade Adams, W. The role of hydrogen bonding in rigid-rod polymers: the crystal structure of a polybenzobisimidazole model compound. *Polymer* **2000**, *41*, 9003−9010.
(39) Musto, P.; Karasz, F. E.; MacKnight, W. J. Hydrogen bonding in polybenzimidazole/polyimide systems: a Fourier-transform infrared investigation using low-molecular-weight monofunctional probes. *Polymer* **1989**, *30*, 1012−1021.
(40) Iwamoto, N. E. *Molecular Modeling Study on the Mechanical Properties of Polybenzimidazole*; NAWCWPNS: 1992.
(41) Ping, Z. H.; Nguyen, Q. T.; Chen, S. M.; Zhou, J. Q.; Ding, Y. D. States of water in different hydrophilic polymers — DSC and FTIR studies. *Polymer* **2001**, *42*, 8461−8467.
(42) Higuchi, A.; Iijima, T. D.s.c. investigation of the states of water in poly(vinyl alcohol) membranes. *Polymer* **1985**, *26*, 1207−1211.
(43) Kim, Y. S.; Dong, L.; Hickner, M. A.; Glass, T. E.; Webb, V.; McGrath, J. E. State of Water in Disulfonated Poly(arylene ether sulfone) Copolymers and a Perfluorosulfonic Acid Copolymer (Nafion) and Its Effect on Physical and Electrochemical Properties. *Macromolecules* **2003**, *36*, 6281−6285.
(44) Roy, A.; Hickner, M. A.; Lee, H.-S.; Glass, T.; Paul, M.; Badami, A.; Riffle, J. S.; McGrath, J. E. States of water in proton exchange membranes: Part A - Influence of chemical structure and composition. *Polymer* **2017**, *111*, 297−306.
(45) Musto, P.; Galizia, M.; Pannico, M.; Scherillo, G.; Mensitieri, G. Time-Resolved Fourier Transform Infrared Spectroscopy, Gravimetry, and Thermodynamic Modeling for a Molecular Level Description of Water Sorption in Poly(e-caprolactone). *J. Phys. Chem. B* **2014**, *118*, 7414−7429.
(46) Lemmon, E. W.; McLinden, M. O.; Friend, D. G. Thermophysical Properties of Fluid Systems. In *NIST Chemistry Webbook, NIST Standard Reference Database Number 69*; Linstrom, P. J., Mallard, W. G., Eds.; National Institute of Standards and Technology: Gaithersburg, MD.
(47) Schult, K. A.; Paul, D. R. Water sorption and transport in blends of polyethyloxazoline and polyethersulfone. *J. Polym. Sci., Part B: Polym. Phys.* **1997**, *35*, 993−1007.
(48) Schult, K. A.; Paul, D. R. Water sorption and transport in blends of poly (vinyl pyrrolidone) and polysulfone. *J. Polym. Sci., Part B: Polym. Phys.* **1997**, *35*, 655−674.
(49) Paul, D. R. Gas Sorption and Transport in Glassy Polymers. *Ber. Bunsenges. Phys. Chem.* **1979**, *83*, 294−302.
(50) Yang, D. K.; Koros, W. J.; Hopfenberg, H. B.; Stannett, V. T. Sorption and transport studies of water in Kapton polymide. I. *J. Appl. Polym. Sci.* **1985**, *30*, 1035−1047.
(51) Akhtar, F. H.; Kumar, M.; Villalobos, L. F.; Shevate, R.; Vovusha, H.; Schwingenschlogl, U.; Peinemann, K.-V. Polybenzimidazole-based mixed membranes with exceptional high water vapor permeability and selectivity. *J. Mater. Chem. A* **2017**, *5*, 21807−21819.
(52) Kamiya, Y.; Hirose, T.; Mizoguchi, K.; Naito, Y. Gravimetric study of high-pressure sorption of gases in polymers. *J. Polym. Sci., Part B: Polym. Phys.* **1986**, *24*, 1525−1539.

DOI: 10.1021/acs.macromol.8b01659
Macromolecules 2018, 51, 7197−7208

(53) Fleming, G. K.; Koros, W. J. Dilation of polymers by sorption of carbon dioxide at elevated pressures. 1. Silicone rubber and unconditioned polycarbonate. *Macromolecules* **1986**, *19*, 2285−2291.
(54) Bevington, P. R.; Robinson, D. K. *Data Reduction and Error Analysis for the Physical Sciences*; McGraw-Hill: Boston, MA, 2003.
(55) Koros, W. J.; Paul, D. R. Sorption and Transport of CO_2 Above and Below Glass Transition of Poly(Ethylene Terephthalate). *Polym. Eng. Sci.* **1980**, *20*, 14−19.
(56) Kelkar, A. J.; Paul, D. R. Water vapor transport in a series of polyarylates. *J. Membr. Sci.* **2001**, *181*, 199−212.
(57) Li, Y.; Nguyen, Q. T.; Buquet, C. L.; Langevin, D.; Legras, M.; Marais, S. Water sorption in Nafion® membranes analyzed with an improved dual-mode sorption model—Structure/property relationships. *J. Membr. Sci.* **2013**, *439*, 1−11.
(58) Stannett, V.; Haider, M.; Koros, W. J.; Hopfenberg, H. B. Sorption and Transport of Water Vapor in Glassy Poly(Acrylonitrile). *Polym. Eng. Sci.* **1980**, *20*, 300−304.
(59) Comesaña-Gandara, B.; Ansaloni, L.; Lee, Y. M.; Lozano, A. E.; De Angelis, M. G. Sorption, diffusion, and permeability of humid gases and aging of thermally rearranged (TR) polymer membranes from a novel ortho-hydroxypolyimide. *J. Membr. Sci.* **2017**, *542*, 439−455.
(60) Chen, G. Q.; Scholes, C. A.; Doherty, C. M.; Hill, A. J.; Qiao, G. G.; Kentish, S. E. Modeling of the sorption and transport properties of water vapor in polyimide membranes. *J. Membr. Sci.* **2012**, *409−410*, 96−104.
(61) Scholes, C. A.; Jin, J.; Stevens, G. W.; Kentish, S. E. Competitive permeation of gas and water vapour in high free volume polymeric membranes. *J. Polym. Sci., Part B: Polym. Phys.* **2015**, *53*, 719−728.
(62) Punsalan, D.; Koros, W. J. Drifts in penetrant partial molar volumes in glassy polymers due to physical aging. *Polymer* **2005**, *46*, 10214−10220.
(63) Galizia, M.; De Angelis, M. G.; Finkelshtein, E.; Yampolskii, Y. P.; Sarti, G. C. Sorption and transport of hydrocarbons and alcohols in addition-type poly(trimethyl silyl norbornene). I: Experimental data. *J. Membr. Sci.* **2011**, *385−386*, 141−153.
(64) Pope, D. S.; Koros, W. J.; Hopfenberg, H. B. Sorption and Dilation of Poly(1-(trimethylsilyl)-1-propyne) by Carbon Dioxide and Methane. *Macromolecules* **1994**, *27*, 5839−5844.
(65) Scherer, J. R.; Bolton, B. A. Water in polymer membranes. 5. On the existence of pores and voids. *J. Phys. Chem.* **1985**, *89*, 3535−3540.
(66) Dlubek, G.; Buchhold, R.; Hübner, C.; Nakladal, A. Water in Local Free Volumes of Polyimides: A Positron Lifetime Study. *Macromolecules* **1999**, *32*, 2348−2355.
(67) Crank, J. *The Mathematics of Diffusion*, 2nd ed.; Oxford University Press: London, 1975.
(68) Long, F. A.; Richman, D. Concentration Gradients for Diffusion of Vapors in Glassy Polymers and their Relation to Time Dependent Diffusion Phenomena. *J. Am. Chem. Soc.* **1960**, *82*, 513−519.
(69) Park, G. S. The Glassy State and Slow Process Anomalies. In *Diffusion in Polymers*; Crank, J., Park, G. S., Eds.; Academic: New York, 1968; pp 141−163.
(70) Morisato, A.; Miranda, N. R.; Freeman, B. D.; Hopfenberg, H. B.; Costa, G.; Grosso, A.; Russo, S. The influence of chain configuration and, in turn, chain packing on the sorption and transport properties of poly(tert-butyl acetylene). *J. Appl. Polym. Sci.* **1993**, *49*, 2065−2074.
(71) Berens, A. R.; Hopfenberg, H. B. Diffusion and relaxation in glassy polymer powders: 2. Separation of diffusion and relaxation parameters. *Polymer* **1978**, *19*, 489−496.
(72) Burgess, S. K.; Mikkilineni, D. S.; Yu, D. B.; Kim, D. J.; Mubarak, C. R.; Kriegel, R. M.; Koros, W. J. Water sorption in poly(ethylene furanoate) compared to poly(ethylene terephthalate). Part 2: Kinetic sorption. *Polymer* **2014**, *55*, 6870−6882.
(73) Doghieri, F.; Sarti, G. C. Solubility, Diffusivity, and Mobility of n-Pentane and Ethanol in Poly(1-trimethylsilyl-1-propyne). *J. Polym. Sci., Part B: Polym. Phys.* **1997**, *35*, 2245−2258.
(74) Minelli, M.; Sarti, G. C. Permeability and diffusivity of CO_2 in glassy polymers with and without plasticization. *J. Membr. Sci.* **2013**, *435*, 176−185.
(75) Minelli, M.; De Angelis, M. G.; Sarti, G. C. Predictive calculations of gas solubility and permeability in glassy polymeric membranes: An overview. *Front. Chem. Sci. Eng.* **2017**, *11*, 405−413.
(76) Galizia, M.; Stevens, K. A.; Paul, D. R.; Freeman, B. D. Modeling gas permeability and diffusivity in HAB-6FDA polyimide and its thermally rearranged analogs. *J. Membr. Sci.* **2017**, *537*, 83−92.
(77) Mi, Y.; Stern, S. A.; Trohalaki, S. Dependence of the gas permeability of some polyimide isomers on their intrasegmental mobility. *J. Membr. Sci.* **1993**, *77*, 41−48.
(78) Coleman, M. R.; Koros, W. J. Isomeric polyimides based on fluorinated dianhydrides and diamines for gas separation applications. *J. Membr. Sci.* **1990**, *50*, 285−297.
(79) Sanders, D. F.; Smith, Z. P.; Guo, R.; Robeson, L. M.; McGrath, J. E.; Paul, D. R.; Freeman, B. D. Energy-efficient polymeric gas separation membranes for a sustainable future: A review. *Polymer* **2013**, *54*, 4729−4761.
(80) Ferrari, M. C.; Galizia, M.; De Angelis, M. G.; Sarti, G. C. Gas and Vapor Transport in Mixed Matrix Membranes Based on Amorphous Teflon AF1600 and AF2400 and Fumed Silica. *Ind. Eng. Chem. Res.* **2010**, *49*, 11920−11935.
(81) Cohen, M. H.; Turnbull, D. Molecular Transport in Liquids and Glasses. *J. Chem. Phys.* **1959**, *31*, 1164−1169.
(82) Park, J. Y.; Paul, D. R. Correlation and prediction of gas permeability in glassy polymer membrane materials via a modified free volume based group contribution method. *J. Membr. Sci.* **1997**, *125*, 23−39.
(83) Bondi, A. van der Waals Volumes and Radii. *J. Phys. Chem.* **1964**, *68*, 441−451.

DOI: 10.1021/acs.macromol.8b01659
Macromolecules 2018, 51, 7197−7208